unoccupied orbitals of A(PL). It is noted that PL used here just refers to an interaction mode that mixes unoccupied orbitals of A into occupied orbitals of A. Hence, the PL interaction may take place to reduce the exchange repulsion as well as to stabilize the electrostatic field of partner molecule B, depending on the relative magnitude of overlap repulsion and electrostatic field. CTPLX(A → B) may have a modified orbital energy gap from CT(A → B) in the energy expression of perturbation expansion. When A is an electron donor and B is an acceptor, CTPLX(A → B) is expected to be larger than CT(A → B) and CTPLX(B → A) may be smaller than CT(B → A). Actually, we have obtained −41, −16, −44, and −54 kcal/mol for FCT, FCTPLX, BCT, and BCTPLX, respectively, for $Ni(PH_3)_2(C_2H_4)$ at $\theta = 26°$.

Concluding Remarks

The bonding between $Ni(PH_3)_2$ and C_2H_4 was analyzed in terms of the donative and the back-donative interactions. The back-donative interaction was proved to be the major contributor to the binding energy as well as to the electron distribution in the complex. Th bent-back structure of coordinated ethylene was shown to be favored due to the favored back-donative interaction. The substitution of PH_3 with NH_3, which is more electron donative, greatly strengthened the back-donative interaction in the $Ni-C_2H_4$ bond. The bonding scheme of $Ni-C_2H_2$ was revealed to be similar to that of $Ni-C_2H_4$, though the magnitude of each energy component was larger in the former than in the latter. The RHF approximation provides a simple model that can describe the bonding nature of transition-metal-olefin complexes, as demonstrated in this work. It is no doubt true, however, that the electron correlation should be taken into account for a more quantitative description of bonding.

Acknowledgment. The authors wish to thank Dr. S. Kato for valuable discussions. Numerical calculations were carried out at the Computer Center of the IMS.

Registry No. $Ni(PH_3)_2(C_2H_4)$, 63995-33-5; $Ni(NH_3)_2(C_2H_4)$, 63995-32-4; $Ni(PH_3)_2(C_2H_2)$, 77342-03-1.

Contribution from the Departments of Chemistry and Physics,
University of Maine, Orono, Maine 04469

Luminescence, Absorption, MCD, and NQR Study of the Cis and Trans Isomers of Dichlorodiammineplatinum(II)

HOWARD H. PATTERSON,* JOHN C. TEWKSBURY, MARILYN MARTIN,
MARY-BETH KROGH-JESPERSEN, JOSEPH A. LoMENZO, HENRY O. HOOPER, and A. KASI VISWANATH

Received July 26, 1979

Luminescence, absorption, magnetic circular dichroism (MCD), and nuclear quadrupole resonance (NQR) experiments are reported for the cis and trans isomers of dichlorodiammineplatinum(II). Extended Hückel molecular orbital calculations, using nonrelativistic and relativistic HF basis functions for Pt, have been made to correlate the experimental data. Analysis of the luminescence intensity and lifetime data vs. temperature for the trans isomer allows us to determine the energy separation of the low-lying triplet d states. The solution MCD spectra indicate the presence of transitions which do not show a maxima in the absorption spectra but which are predicted from the MO calculations. The ^{35}Cl NQR results for the cis and trans isomers allow a comparison of the ground electronic state chemical bonding for the two isomers; also, since the NQR coupling constant MO calculations are a more sensitive test of the MO wave functions than energy calculations, the NQR data can be used to judge our MO models.

Introduction

In a series of studies[1-6] we have reported the absorption and luminescence spectra of selected platinum complexes. In this paper we consider the cis and trans isomers of dichlorodiammineplatinum(II). The cis isomer is of current interest because of its anticancer activity. ^{35}Cl NQR measurements have been made to probe the ground electronic state bonding while luminescence, MCD, and absorption measurements have been used to determine the excited electronic state ordering in both solution and solid-state environments.

Previously Chatt et al.[7] have reported the solution spectra of *cis*- and *trans*-$Pt(NH_3)_2Cl_2$ and assigned the low-energy transitions as d-d on the basis of the extinction coefficients. Also, Martin and co-workers[8,9] have reported the solution and polarized single-crystal absorption spectra of $Pt(en)Cl_2$ and discovered significant differences int the two spectra. These differences were assigned to the presence of inter- and intramolecular excitonic transitions in the solid state. Recently, Martin et al.[10] have compared the $Pd(en)Cl_2$ spectra with the platinum results.

Experimental Methods

cis-$Pt(NH_3)_2Cl_2$ was prepared by the method of Dhara.[11] K_2PtCl_4 was converted to K_2PtI_4 and then to *cis*-$Pt(NH_3)_2I_2$ by addition of NH_4OH. Reaction with $AgNO_3$ produced *cis*-$[Pt(NH_3)_2(H_2O)_2](NO_3)_2$, which upon addition of KCl produced the final product. Purification was accomplished by successive recrystallization from a 0.1 N HCl solution. The *trans*-$Pt(NH_3)_2Cl_2$ isomer was prepared with use of the method of Kauffman and Cowan.[12] The product was purified from 0.1 N HCl.

In order to obtain luminescence spectra in the limit of zero Pt-Pt interaction, we rapidly froze solutions containing the cis or trans

---

(1) H. H. Patterson, J. J. Godfrey, and S. M. Khan, *Inorg. Chem.*, **11**, 2872 (1972).
(2) T. G. Harrison, H. H. Patterson, and J. J. Godfrey, *Inorg. Chem.*, **15**, 1291 (1976).
(3) H. H. Patterson, T. G. Harrison, and R. J. Belair, *Inorg. Chem.* **15**, 1461 (1976).
(4) T. G. Harrison, H. H. Patterson, and M. T. Hsu, *Inorg. Chem.*, **15**, 3018 (1976).
(5) H. H. Patterson, W. J. DeBerry, J. E. Byrne, M. T. Hsu, and J. A. LoMenzo, *Inorg. Chem.*, **16**, 1698 (1977).
(6) M. Laurent, J. C. Tewksbury, M. B. Krogh-Jespersen, and H. H. Patterson, *Inorg. Chem.*, **19**, 1656 (1980).
(7) J. Chatt, G. A. Gamlen, And L. E. Orgel, *J. Chem. Soc.*, 486 (1958).
(8) D. S. Martin, Jr., L. D. Hunter, R. Kroening, and R. F. Coley, *J. Am. Chem. Soc.*, **93**, 5433 (1971).
(9) D. S. Martin, Jr., *Inorg. Chim. Acta, Rev.*, **5**, 107 (1971).
(10) D. S. Martin, Jr., G. A. Robbins, and R. M. Rush, *Inorg. Chem.*, **19**, 1705 (1980).
(11) S. C. Dhara, *Indian J. Chem.*, **8**, 193 (1970).
(12) G. B. Kauffman and B. O. Cowan, *Inorg. Synth.*, **7**, 242 (1963).

0020-1669/81/1320-2297$01.25/0

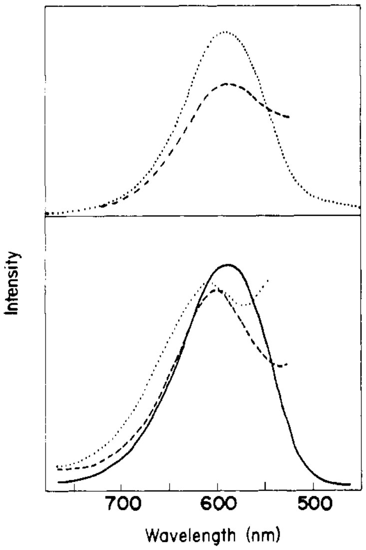

Figure 1. Luminescence spectra of the cis (top figure portion) and trans (bottom figure portion) isomers of dichlorodiammineplatinum(II) at 78 K: —, KBr; ···, Me_2SO; - - -, DMF.

isomers. Approximately 2 mL of the compound of interest in DMF or Me_2SO solvent was poured into the bottom of a quartz Dewar. Liquid nitrogen was then carefully poured on top of this solution, causing it to solidify quickly and trap the guest within the crystal lattice of the host.

The initial luminescence measurements were recorded on a Perkin-Elmer MPF-44A spectrophotometer utilizing a 120-W xenon lamp and a HTV-R477 Na-K-Sb-Cs photomultiplier tube as a detector. Temperature-dependent luminescence measurements were carried out with a $^3/_4$-m McPherson monochromator coupled to a PAR Research Model 124A lock-in amplifier using an RCA-C7151U-RF photomultiplier tube and a Soltec B-181 recorder. The sample was cooled with an Air Products Cryo-Tip heat exchanger, Model No. AC-31-110. Lifetime studies were done a Molectron Corp. UV 14 Series II pulsed nitrogen laser using a Model 162 PAR Boxcar integrator. Lifetimes longer than 10 ns can be measured with this setup.

The absorption experiments were carried out on a Cary 17DX extended range spectrophotometer with a LT-3-110 liquid-helium transfer Heli-Tran. The MCD instrument was a Cary 60 spectrapolarimeter with a Cary MCD accessory and a Westinghouse 60-Kg superconducting magnet.

NQR studies were made with a continuous superregenerative oscillator with narrow band amplification, phase detection, and subsequent display of resonance data on a strip chart recorder. The apparatus was operated at room temperature and at liquid-nitrogen temperature. The signal observed for the *cis*-$Pt(NH_3)_2Cl_2$ isomer was very weak at 78 K.

Luminescence of *cis*- and *trans*-$Pt(NH_3)_2Cl_2$

The luminescence of *cis*- and *trans*-$Pt(NH_3)_2Cl_2$ in frozen solvent lattices of dimethyl sulfoxide (Me_2SO) and dimethylformamide (DMF) at 78 K are shown in Figure 1. The origin of the cis isomer in Me_2SO occurs at 23 800 cm^{-1} (420 nm), approximately the same energy where the solution absorption spectrum shows zero absorbance; also, the luminescence maximum occurs at 16 950 cm^{-1} (590 nm). In contrast, the trans isomer luminescence maximum is at 16 400 cm^{-1} (610 nm) in Me_2SO and at 16 500 cm^{-1} in DMF. The disadvantage of using Me_2SO or DMF as frozen solvents is that they show fluorescence in the high-energy end of the diamine luminescence spectrum and complicate any study of the temperature dependence of the amine luminescence. However, the solvent fluorescence state is also probably responsible for efficient energy transfer to the lower energy platinum excited states to give enhanced ammine luminescence in the Me_2SO and DMF solvents.

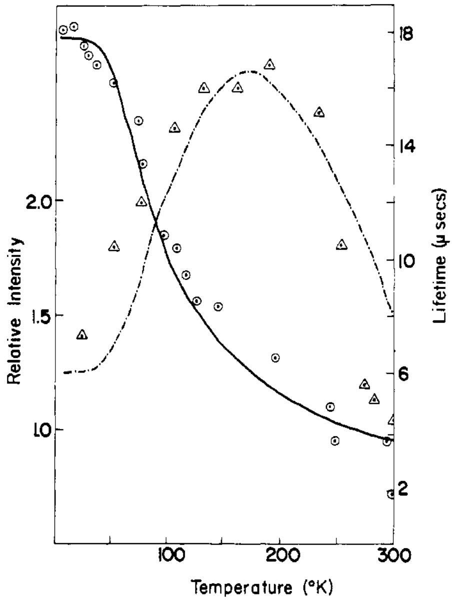

Figure 2. Variation of the luminescence intensity (triangles) and lifetime (circles) with temperature for *trans*-dichlorodiammineplatinum(II) in a KBr pellet. The lines shown are the calculated results for the three state models described in the text.

Luminescence vs. temperature data was recorded for only the trans isomer in KBr pellets with the intensity weaker than that observed with Me_2SO and DMF solvents. Luminescence of the cis isomer in KBr was too weak to be detected. Figure 2 shows a plot of the relative luminescence intensity vs. temperature for *trans*-$Pt(NH_3)_2Cl_2$. An initial increase of intensity occurs as the temperature of the trans sample is cooled to about 200 K, and then there is a constant decrease in intensity as the temperature is lowered further. Also, in Figure 2 we show the variation of luminescence lifetime with temperature from 300 to 5 K.

We have analyzed the temperature dependence of the trans-luminescence intensity and lifetime data as follows. Upon pulsed laser excitation of a sample, the decay rate is given by eq 1,[13] where N is the total population of excited

$$\frac{dN}{dt} = -\frac{1}{\tau}N = -\sum_{i=1}^{n}(K_{ir} + K_{iv})n_i \qquad (1)$$

electronic states, n_i is the population of the ith excited state, and K_{ir} and K_{iv} are the radiative and nonradiative rate constants for the depopulation of the ith excited state. Three models have been considered to describe the lifetime and intensity variation with temperature: (1) a two-state emission model with temperature-independent decay processes; (2) a three-state emission model with temperature-independent decay processes; (3) a two-state emission model in which the nonradiative rate constants (K_{iv}) have the temperature dependence of eq 2.[14] The lifetime and intensity vs. temperature

$$K_{iv} = K_{ia} + K_{ib}\exp(-E_A/KT) \qquad (2)$$

data were fit by each of the three models with the use of a simplex method. The model which gave the best fit to the experimental data of Figure 2 was the three-state temperature-independent emission model. The calculated energies of the three emitting excited states were 0, 157, and 337 cm^{-1} with radiative rate constants of 0.04, 0.05, and 0.002 μs^{-1}, in contrast to values, respectively, of ($K_{ir} + K_{iv}$) of 0.057, 0.50, and 1.30 μs^{-1}.

NQR, MCD, and Absorption Results

Molecular Orbital Model. Extended Hückel molecular orbital calculations were performed for both the *cis*- and

---

(13) G. D. Hager and G. A. Crosby, *J. Am. Chem. Soc.*, **97**, 7031 (1975).
(14) R. Engleman and J. Jortner, *Mol. Phys.*, **18**, 145 (1970).

Table I. NQR Results for Cis and Trans Platinum Amine Complexes

compd	2ν (e^2qQ, MHz)
cis-$Pt(NH_3)_2Cl_2$	32.36 (77 K)
trans-$Pt(NH_3)_2Cl_2$	34.60[a] (273 K) 34.86 (300 K) 36.62 (77 K)
cis-$Pt(MeNH_2)_2Cl_2$	34.42[a] (273 K)
trans-$Pt(MeNH_2)_2Cl_2$	36.32[a] (273 K)

[a] Data from C. W. Fryer and J. A. S. Smith, *J. Chem. Soc. A*, 1029 (1970).

Table II. NQR Molecular Orbital Calculations for Cases I, II and III

calculation	% s	–Cl charge[a]	e^2qQ-(T-D),[b] MHz	e^2qQ-(C-H),[c] MHz	η[d]
		cis-$Pt(NH_3)_2Cl_2$			
single STO	23	0.62	32	35	0.14
nonrel LCSTO	56	0.63	18	25	0.50
rel LCSTO	51	0.65	19	25	0.41
		trans-$Pt(NH_3)_2Cl_2$			
single STO	19	0.60	36	36	0.13
nonrel LCSTO	57	0.62	18	26	0.47
rel LCSTO	52	0.64	19	26	0.38

[a] Chlorine charge used was from the molecular orbital results. [b] e^2qQ(T-D): Townes and Dailey formalism. [c] e^2qQ(C-H): Cotton and Harris molecular orbital formalism. [d] η: asymmetry parameter.

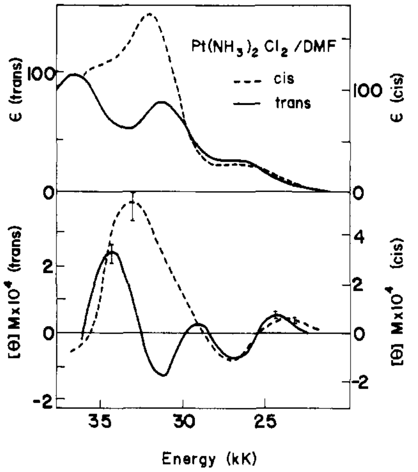

Figure 3. Room-temperature solution absorption (top figure portion) and MCD (bottom figure portion) spectra for the cis and trans isomers of dichlorodiammineplatinum(II).

trans-dichlorodiammineplatinum(II) complexes.

A total of 31 atomic orbitals were considered in our calculation: Pt^0 (5d,6s,6p), N^0 (2s,2p), Cl^0 (3s,3p) and H^0 (1s). Nitrogen radial functions were generated with the use of Herman–Skillman potentials[15] in a Hartree–Fock–Slater self-consistent-field (HFS-SCF) calculation. Wave functions generated in this manner are normalized and have the correct number of radial nodes. Chlorine orbitals of the same type, fit to a linear combination of STO's, were taken from Watson and Freeman.[16]

Molecular configurations and bond lengths were taken from Milburn and Truter.[17] Although some distortion from a square-planar coonfiguration occurs in the solid state for both isomers, the assumption was made that all platinum ligand bond angles are 90°. Since no data was available for N–H bond angles or lengths, the assumption was made that the bonding geometry was tetrahedral with H–N–H bond angles of 109.5° and bond lengths the same as those with ammonia.

Platinum wave functions of three different types were used. First, in case I, single STO's were taken from Cotton and Harris.[18] These functions are, of course, nodeless and were determined by variation of the shielding constant until overlap values were consistent with those obtained from SCF functions. Second, in case II, nonrelativistic platinum wave functions were generated from a HFS-SCH calculation, as with nitrogen. The 6s and 6p functions had to be obtained with use of the excited states $5d^96s^16p^0$, $5d^96s^06p^1$, or $5d^86s^16p^1$. Finally, for case III, relativistic platinum functions were generated at Brookhaven National Laboratory with use of the relativistic Hartree–Fock program[19] INGVAR. Here again, excited states had to be used to obtain the 6s and 6p wave functions.

All radial wave functions generated via HFS-SCF or INGVAR were fit to a linear combination of STO's of the form of eq 3 and normalized with r in atomic units. A discussion of one way to carry out this fit has been given previously.[20]

$$\Psi(r) = \sum_i C_i r^{n_i} \exp(-\alpha_i r) \qquad (3)$$

^{35}Cl NQR Results. In Table I we summarize our experimental ^{35}Cl NQR results for the *cis*- and *trans*-$Pt(NH_3)_2Cl_2$ isomers.[21] Using the Townes and Dailey relation[22] (eq 4) with

$$(e^2qQ_{\text{mol}})/(e^2qQ_{\text{at}}) = (1 - S)(1 - i) \qquad (4)$$

the usual assumption of 15% s hybridization yields a charge on Cl for the cis and trans isomers of –0.65 and –0.63, respectively. This is in agreement with the Townes and Dailey calculated results for $Pt(MeNH_2)_2Cl_2$ cis and trans isomers.[21]

In Table II we summarize our NQR coupling constant predictions using our MO results. To estimate e^2qQ from eq 4 we estimate the % s hybridization by eq 5 where $\sum\sigma_{\text{Cl(s)}}$ is

$$S = \sum\sigma_{\text{Cl(s)}}/\sum\sigma_{\text{Cl}} \qquad (5)$$

the sum of the σ overlap populations involving the chlorine s orbital and $\sum\sigma_{\text{Cl}}$ is the sum of all overlap populations involving σ bonding to platinum. The Cotton and Harris MO formalism was also used to estimate e^2qQ. From the Table II results we conclude that the single STO of Cotton and Harris (case I) best predicts e^2qQ for both the *cis*- and *trans*-$Pt(NH_3)_2Cl_2$ isomers. We find from the case I results that the % s hybridization for both isomers is about 20% with the Cl charge slightly more negative in the cis isomer case.

MCD and Absorption Solution Results. The MCD and the absorption spectra of the cis and trans isomers are given in Figure 3. DMF was the solvent of choice because of the relative insolubility of either isomer in dilute HCl. The MCD spectra were fit to a linear combination of Gaussian functions (eq 6) by a least-squares computer program. $\nu_K{}^\circ$ is the peak

$$f = \sum_K I_K \exp(-\alpha_K(\nu - \nu_K{}^\circ)^2) \qquad (6)$$

---

(15) F. Herman and S. Skillman, "Atomic Structure Calculations", Prentice-Hall, Englewood Cliffs, NJ, 1963.
(16) R. E. Watson and A. J. Freeman, *Phys. Rev.*, **123**, 521 (1961).
(17) G. H. W. Milburn and M. R. Truter, *J. Chem. Soc. A*, 1610 (1966).
(18) F. A. Cotton and C. B. Harris, *Inorg. Chem.*, **6**, 369 (1967).
(19) E. W. McDaniel and M. R. C. McDowell, Eds., "Case Studies in Atomic Physics", Vol. 4, North-Holland Publishing Co., Amsterdam, 1975.
(20) T. G. Harrison, Masters Thesis, University of Maine, 1975.
(21) C. W. Fryer and J. A. S. Smith, *J. Chem. Soc. A*, 1029 (1970).
(22) C. N. Townes and B. P. Dailey, *J. Chem. Phys.*, **17**, 782 (1949).
(23) F. A. Cotton and C. B. Harris, *Proc. Natl. Acad. Sci. U.S.A.*, **56**, 12 (1966).

Table III. Assignment of the Visible-UV Absorption and MCD Spectra[a] of *cis*- and *trans*-Pt(NH$_3$)$_2$Cl$_2$

energy, cm^{-1}				
absorption	MCD	ϵ, cm^{-1} M^{-1}	$10^4 \times [\Theta]_M$	assignt
				(a) Cis Isomer
	23 700		+0.6	($^3B_1$, $^3A_2$) $d_{xy} \leftarrow d_{xz},d_{yz}$
27 000	27 100	25	−1.2	($^3B_2$) $d_{xy} \leftarrow d_{x^2-y^2}$
	30 500		+0.9	($^3B_2$) $d_{xy} \leftarrow d_{z^2}$
32 500	33 200	170	+5.4	($^1B_2$) $d_{xy} \leftarrow d_{x^2-y^2}$
35 500		110		($^1A_2$) $d_{xy} \leftarrow d_{yz}$ ($^1B_1$) $d_{xy} \leftarrow d_{xz}$
45 500[b]		2000		($^1B_1$) $6p_z \leftarrow d_{x^2-y^2}$ ($^1A_1$) $6p_z \leftarrow d_{yz}$
49 500[b]		7500		($^1B_2$) $6p_z \leftarrow d_{xz}$
				(b) Trans Isomer
	24 600		+0.6	($^3B_{2g}$, $^3B_{3g}$) $d_{x^2-y^2} \leftarrow d_{xz},d_{yz}$
26 900	27 000	30	−0.8	(^3B_g) $d_{x^2-y^2} \leftarrow d_{xy}$
	29 000		+0.5	(^3A_g) $d_{x^2-y^2} \leftarrow d_{z^2}$
31 700	31 400	75	−1.2	($^1B_{1g}$) $d_{x^2-y^2} \leftarrow d_{xy}$
	34 400		+2.0	($^1B_{2g}$) $d_{x^2-y^2} \leftarrow d_{xz}$
36 700		100		($^1B_{3g}$) $d_{x^2-y^2} \leftarrow d_{yz}$
46 500[b]		2700		($^1B_{3u}$) $6p_z \leftarrow d_{xz}$
50 000[b]		6500		($^1B_{2u}$) $6p_z \leftarrow d_{yz}$

[a] MCD peak positions were determined by Gaussian analysis.
[b] Assignment of these peaks is based on case I.

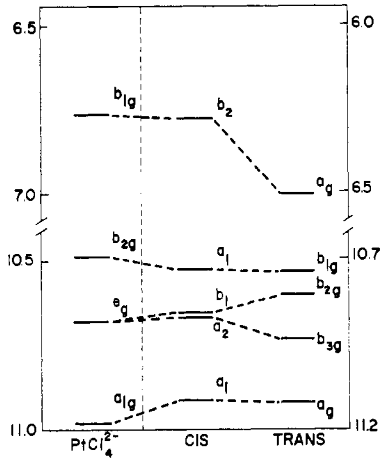

Figure 4. Extended Hückel molecular orbital calculated results for the cis and trans isomers fo dichlorodiammineplatinum(II) in comparison with the tetrachloroplatinate(II) ion. The labels for the electronic levels are the irreducible representations according to which the electronic states transform.

position, I_K is the intensity, and α_K is a constant related to the half-width $\nu_{1/2}$ by eq 7. Gaussian fit results for the MCD spectra are given Table III.

$$\alpha_K = -2.773/\nu_{1/2}^2 \qquad (7)$$

The results of our molecular orbital calculations for PtCl$_4^{2-}$, *cis*-Pt(NH$_3$)$_2$Cl$_2$, and *trans*-Pt(NH$_3$)$_2$Cl$_2$ are shown in Figure 4. This cis isomer and PtCl$_4^{2-}$ results are very similar. From these MO calculations the cis isomer absorption maximum at 32 500 cm^{-1} (ϵ 170 cm^{-1} M^{-1}) is assigned as $d_{x^2-y^2} \rightarrow d_{xy}$ ($^1B_2$). The peak at 35 500 cm^{-1} (ϵ 110 cm^{-1} M^{-1}) is assigned to a combination of $d_{xz} \rightarrow d_{xy}$ ($^1B_1$) and $d_{yz} \rightarrow d_{xy}$ ($^1A_2$) transitions since the MO calculations predict these two transitions to be unresolvable in the solution spectrum. The transition $d_{z^2} \rightarrow d_{xy}$ ($^1B_2$), although not visible in the solution spectrum, is expected to lie under the charge-transfer bands.

In Figure 5 is shown the cis-isomer absorption spectrum recorded in water within 5 min of dissolution. For the assignment of these low-lying charge-transfer bands, our MO results are inconsistent among cases I, II, and III. MCD data[24] and single-crystal reflectance measurements[25] for PtCl$_4^{2-}$ indicates the low-lying charge-transfer transitions to be d → p_z. This is consistent with our case I MO results. Therefore, the shoulder at 45 500 cm^{-1} (ϵ 2000 cm^{-1} M^{-1}) and the band at 49 500 cm^{-1} (ϵ 7500 cm^{-1} M^{-1}) are tentatively assigned as d → p_z transitions.

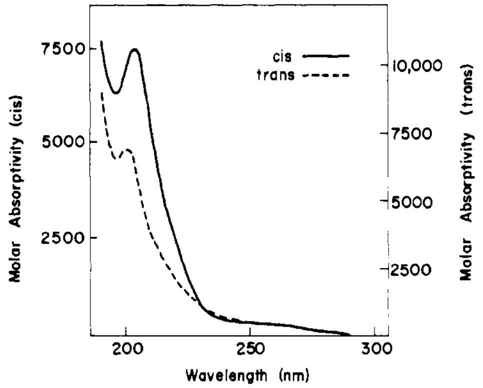

Figure 5. Room-temperature aqueous UV absorption spectra of the two Pt(NH$_3$)$_2$Cl$_2$ isomers showing the allowed charge-transfer transitions.

The low-intensity cis-isomer bands at energies less than 31 000 cm^{-1} are assigned to singlet–triplet d–d transitions. Since the energy difference between the observed singlet excited states is the same in PtCl$_4^{2-}$ ($^1A_{2g}$ and ^1E_g states)[1] as with the cis isomer (3.5 × 10^3 cm^{-1}) it is reasonable to expect that the corresponding triplet states will show the same relative energies. We predict that the cis(d_{xz}, d_{yz}) and d_{xy} triplet states will occur at 24.0 × 10^3 and 27.1 × 10^3 cm^{-1} in comparison to 17.6 × 10^3 and 20.7 × 10^3 cm^{-1} for PtCl$_4^{2-}$. The observed peaks for the cis isomer at 23.7 × 10^3, 27.1 × 10^3 and 30.5 × 10^3 cm^{-1} are, thus, assigned to singlet–triplet transitions involving d_{xz}, $d_{yz} \rightarrow d_{xy}$, $d_{x^2-y^2} \rightarrow d_{xy}$ and $d_{z^2} \rightarrow d_{xy}$, respectively.

For the trans isomer the band at 31 400 cm^{-1} is assigned as $d_{xy} \rightarrow d_{x^2-y^2}$ ($^1B_{1g}$). Its apparent weakness may be a result of the superposition of a negative MCD peak below a weaker positive peak. The unexpected MCD band at 34 000 cm^{-1} corresponds to a minimum in the absorption spectrum and reveals the presence of an additional transition not seen in the absorption spectrum. It is assigned to a singlet–singlet transition because of its intensity and because of its position well within the other d–d spin-allowed bands. This band is assigned from our MO results to the transition $d_{xz} \rightarrow d_{x^2-y^2}$ ($^1B_{2g}$). The band at 36 000 cm^{-1} is assigned to the transition $d_{yz} \rightarrow d_{x^2-y^2}$ ($^1B_{3g}$). The observed singlet–triplet transitions at about 24 600, 27 000, and 29 000 cm^{-1} are assigned as for the cis isomer to d_{xz}, $d_{yz} \rightarrow d_{x^2-y^2}$, $d_{xy} \rightarrow d_{x^2-y^2}$, and $d_{z^2} \rightarrow d_{x^2-y^2}$, respectively. Our trans-luminescence analysis indicates the three lowest d_{xz}, $d_{yz} \rightarrow d_{x^2-y^2}$ components have relative energies of 0, 157, and 337 cm^{-1}.

Solid-State Absorption Spectra. The absorption spectrum for the cis isomer (Figure 6) in KBr shows a band at 25 600 cm^{-1}, a shoulder at 32 300 cm^{-1} and a band around 37 000 cm^{-1}. The band at 37 000 cm^{-1} becomes narrower and shifted to lower energies upon cooling. The shoulder at 32 300 cm^{-1} shows little apparent temperature dependence down to 7 K. These bands are therefore assigned to electric-dipole-allowed transitions. In contrast, the region of the spectrum between 32 300 and 18 000 cm^{-1} with cooling shows a slight decrease

---

(24) A. J. McCaffery, P. N. Schatz and P. J. Stephens, *J. Am. Chem. Soc.*, **90**, 5730 (1968).

(25) B. G. Anex and N. Takeuchi, *J. Am. Chem. Soc.*, **96**, 4411 (1974).

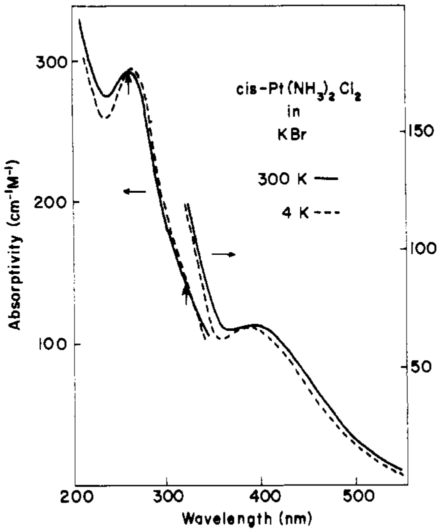

Figure 6. Temperature variation of the absorption spectra of a KBr pellet containing *cis*-$Pt(NH_3)_2Cl_2$. The two regions indicated by arrows at about 32 000 and 37 000 cm^{-1} show some allowed character since the absorption here shows no decrease in magnitude with decreasing temperature.

in intensity along with a distinct narrowing and a slight shift to higher energies. These features are characteristic of vibronically allowed d–d bands.

Extended Hückel molecular orbital calculations on dimers and trimers of *cis*-$Pt(NH_3)_2Cl_2$ (Figure 7) show that as the intermolecular Pt–Pt distance is shortened the energies of the d orbitals remain constant. However, the $6p_z$ orbital becomes lower in energy and the Cl π orbitals increase in energy. As a result, we find that in the pure crystal case the charge-transfer transitions move to lower energies and become comparable in energy to the d–d transitions. The bands at 32 300 and 37 000 cm^{-1} are assigned to $d_{z^2} \rightarrow 6p_z$ and L $\pi \rightarrow d_{xy}$ transitions.

The solid-state absorption spectrum of *trans*-$Pt(NH_3)_2Cl_2$ in KBr pellets shows a shoulder at 27 000, another at 32 300, and a peak at 43 500 cm^{-1}. These peaks match quite closely in energy and relative intensity with the peaks in the solution spectrum. The temperature-dependent absorption spectrum shows that all three bands decrease in intensity and shift to higher energies as the temperature is decreased from 300 to 7 K. Therefore, the spectrum in the solid consists of d–d bands only. The MO calculations for trans dimers with a Pt–Pt spacing of 5.0 Å show little intermolecular interaction between the orbitals in agreement with our experimental results.

Summary

In this paper we have discussed the interpretation of a series of spectroscopic experiments on the cis and trans isomers of $Pt(NH_3)_2Cl_2$. Luminescence, absorption, and MCD experiments have been used to characterize the excited electronic states while NQR has been used to probe the electronic ground state for the two isomers.

The cis isomer shows luminescence at higher energies ($\sim$16 950 cm^{-1}) than the trans isomer ($\sim$16 400 cm^{-1}), with the trans luminescence about 100 times more intense than the cis. The trans isomer has D_{2h} symmetry and a center of symmetry unlike the cis isomer, and this is thought to be responsible for the difference in relative intensity. A microscopic analysis of the temperature-dependent luminescence intensity and lifetime data for the trans isomer indicate the lowest excited states to be at relative energies of about 0, 160, and 340 cm^{-1}.

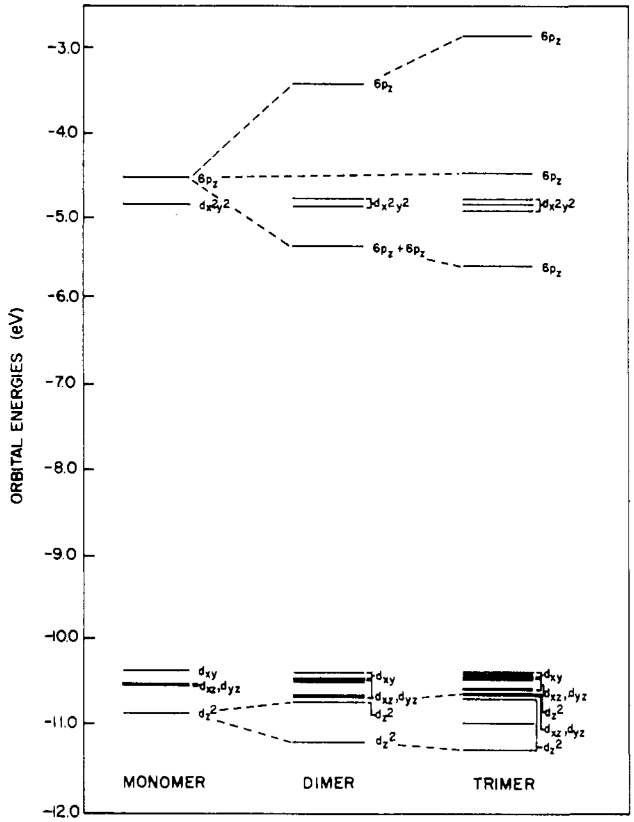

Figure 7. Extended Hückel molecular orbital calculations for a monomer, dimer, and trimer of *cis*-dichlorodiammineplatinum(II) oriented as in a crystal. Extrapolation of these results to the polymer case yields a band description of the isomer. In this case, transitions can occur between filled bands and empty bands for *K* values where there is a sufficient density of allowed states for both the initial and final bands.

The absorption and MCD spectra of the two isomers allows assignments in the two cases. For the cis isomer, the excited electronic states are remarkably similar to the $PtCl_4^2$ excited electronic states in relative energy but uniformly at about 6 $\times$ 10^3 cm^{-1} higher energy. In contrast for the trans isomer, the *xz* and *yz* degeneracies are removed and the resulting singlet states are split by about 1400 cm^{-1}; also, the effect of this loss of degeneracy is shown in the trans-luminescence change with temperature. For both isomers, our MO calculations are able to provide reasonable models.

The NQR ^{35}Cl results are particularly interesting because they can be used to show more covalent bonding in the Pt–Cl trans isomer than for the Pt–Cl cis isomer. The Cl cis charge is about −0.62 while the Cl trans charge is about −0.60. Molecular orbital calculations with nonrelativistic HF or relativistic HF wave functions for Pt give exactly the same relative ordering of the d orbitals and, thus, predict the same d–d electronic spectra but show differences in the relative energies of the d $\rightarrow$ p and Cl $\pi \rightarrow$ d transitions. However, the Cl NQR coupling constants calculated with use of either, a Townes–Dailey formalism or a Cotton–Harris MO approach are in good agreement with experiment for only the Cotton–Harris single-Slater representation for the Pt wave functions. These results suggest that NQR results can be a sensitive criteria for comparing MO models.

Acknowledgment. This research was supported by the Americal Cancer Society.

Registry No. *cis*-$Pt(NH_3)_2Cl_2$, 15663-27-1; *trans*-$Pt(NH_3)_2Cl_2$, 14913-33-8.